Journal of Power Sources 196 (2011) 5470–5477

Contents lists available at ScienceDirect

Journal of Power Sources

journal homepage: www.elsevier.com/locate/jpowsour

Poly(styrene sulfonic acid)/poly(vinyl alcohol) copolymers with semi-interpenetrating networks as highly sulfonated proton-conducting membranes

Chun-En Tsai [a], C.W. Lin [b], John Rick [a], Bing-Joe Hwang [a,c,*]

[a] Nanoelectrochemistry Laboratory, Department of Chemical Engineering, National Taiwan University of Science and Technology, Taipei 106, Taiwan
[b] Department of Chemical Engineering, National Yunlin University of Science and Technology, Yunlin, Taiwan
[c] National Synchrotron Radiation Research Center, Hsinchu 300, Taiwan

ARTICLE INFO

Article history:
Received 5 October 2010
Received in revised form 8 January 2011
Accepted 10 January 2011
Available online 19 January 2011

Keywords:
Semi-interpenetrating network
Poly(vinyl alcohol)
Proton conducting membrane
Sulfonation
Two-step crosslinking process

ABSTRACT

Poly(styrene sulfonic acid)/poly(vinyl alcohol) proton-conducting membranes with semi-interpenetrating networks (semi-IPNs) were prepared using a modified two-step crosslinking strategy. We previously employed sulfosuccinic acid (SSA) and glutaraldehyde (GA) as crosslinking agents to form a dense hydrophobic layer at the outer membrane surface. Although the proton conductivity of the resulting membrane increased with the content of SSA, the methanol permeability also increased. In this study it was found that the introduction of a sufonating agent, with a high molecular weight, i.e. poly(styrene sulfonic acid) (PSSA), at a PSSA/poly(vinyl alcohol) ($g\,g^{-1}$) ratio greater than 0.72, increased the density of the tangled IPN structures that effectively impede the membrane's permeability to MeOH, while enhancing its proton conductivity. The synthesized semi-IPN membranes exhibited high proton conductivities (up to $5.88 \times 10^{-2}\,S\,cm^{-1}$ at room temperature, i.e. greater than those of Nafion membranes) and high resistances to MeOH permeation (ca. $1 \times 10^{-7}\,cm^2\,S^{-1}$, that is approximately one order of magnitude lower than that of Nafion membranes).

© 2011 Elsevier B.V. All rights reserved.

1. Introduction

Fuel cells are potential contributors to the next-generation of clean energy sources. Several types of fuel cells, e.g. hydrogen and direct methanol fuel cells (DMFCs), utilize proton conducting membranes. The perfluorinated ionomer Nafion is commonly employed as an electrolyte in hydrogen and direct methanol fuel cells. Nafion, which features a poly(tetrafluoroethylene) backbone presenting perfluorinated pendent chains terminated by sulfonic acid units, offers exceptional: chemical, thermal, and mechanical stability, together with high proton conductivity. Nevertheless, the high cost of Nafion's cell components, its instability at high temperatures, and its high methanol (MeOH) permeability hinder its widespread applicability [1–3]. To reduce the permeability (cross-over) of the fuel (MeOH) in DMFCs, from the anode side of the membrane to the cathode side, the solid polymer electrolyte membrane in a DMFC must act as a barrier [4].

Channel structures in membranes, comprising hydrated perfluorosulfonic acid polymers, exhibit high proton conductivities; however, due to its affinity to water, MeOH is also able to readily pass through the membranes, thus limiting their barrier properties [4]. Previous research has led to the development of a highly proton-conducting Nafion/$-SO_3H$ functionalized mesoporous silica composite-membrane exhibiting a MeOH permeability of $4.5 \times 10^{-6}\,cm^2\,S^{-1}$ [5]. Other researchers have used sulfonation agents, such as sulfoacetic acid, 4-sulfophthalic acid, and sulfosuccinic acid (SSA), all of which possess both sulfonic and carboxylic acid groups, as crosslinking agents to prepare poly(vinyl alcohol) (PVA)-based solid polymer electrolytes [6,7]. Organic/inorganic hybrid membranes containing sulfonic acid groups, introduced using various sulfonation agents, have also been prepared using sol–gel processes under acidic conditions [8–11]. Another study found that PVA/SSA/silica hybrid membranes containing various SSA contents had MeOH permeabilities ranging from 10^{-8} to $10^{-7}\,cm^2\,S^{-1}$ and proton conductivities ranging from 10^{-3} to $10^{-2}\,S\,cm^{-1}$ [10]. Crosslinked PVA/SSA/poly(acrylic acid) (PAA)/silica hybrid membranes have also been prepared using a chemical crosslinking agent containing an SO_3H group; this approach increases the proton conductivity (from 10^{-3} to $10^{-2}\,S\,cm^{-1}$) while simultaneously decreasing the MeOH permeability (from 10^{-8} to $10^{-7}\,cm^2\,S^{-1}$) [11].

Polymer family membranes have also been prepared and evaluated as proton-conducting materials on the basis of binary chemical crosslinking [12]. As an example of this

* Corresponding author at: Nanoelectrochemistry Laboratory, Department of Chemical Engineering, National Taiwan University of Science and Technology, #43, Keelung Rd., Sec. 4, Taipei 106, Taiwan. Tel.: +886 2 27376624; fax: +886 2 27376644.
E-mail address: bjh@mail.ntust.edu.tw (B.-J. Hwang).

0378-7753/$ – see front matter © 2011 Elsevier B.V. All rights reserved.
doi:10.1016/j.jpowsour.2011.01.020

approach, a semi-interpenetrating polymer network (semi-IPN) has been formed from a two-polymer composite, comprising the proton-conducting polymer poly(2-acrylamido-2-methyl-1-propanesulfonic acid) (PAMPS) and PVA, which was reacted with a dialdehyde to form a crosslinking structure that served as a MeOH barrier with the ionic conductivity and the MeOH permeability being controlled by adjustment of the polymer ratio and the extent of crosslinking [12–14]. Proton exchange membranes have also been prepared using blends of PVA and poly(styrene sulfonic acid-*co*-maleic acid) (PSSA-MA) [15,16]. Other semi-IPNs have been based on the crosslinking of PVA with SSA and by the use of PSSA-MA as a proton source to form a semi-IPN PVA/SSA/PSSA-MA membrane [17,18]. The use of SSA as the crosslinking agent simultaneously increases the proton conductivity and reduces the MeOH permeability of PVA-based polymer electrolyte membranes. Unfortunately, these esterized crosslinking bonds are readily hydrolyzed by acids. The single/bridge esterization ratio between PVA and SSA molecules increases with respect to the amount of SSA [7]. A PVA/SSA membrane will dissolve in water when the content of the SSA crosslinking agent exceeds ca. 10 mol% based on PVA-OH. PVA/SSA/silica organic/inorganic hybrid membranes have lower proton conductivities than the corresponding pure organic PVA/SSA membranes, and the use of inorganic silica readily induces phase separation. Such organic/inorganic hybrid membranes become brittle and cracked when a large amount of SSA crosslinking agent or silica is employed [8–11]. Semi-IPNs composed of PVA/PAMPS, crosslinked with a dialdehyde, exhibit high MeOH permeabilities [12–14]. The above examples show that the one-step cross-linking strategies commonly employed tend to produce electrolyte membranes that exhibit either lower proton conductivity, or a lower MeOH permeability barrier.

In our previous work, PVA based proton conducting membranes were prepared by using a two-step crosslinking strategy that involved esterization and acetal formation [19]. We used sulfosuccinic acid (SSA) as the first crosslinking agent to form an inter-crosslinked structure, after which glutaraldehyde (GA) was employed as the second crosslinking agent to form a dense and hydrophobic layer at the membrane's outer surface. It was found that although the proton conductivity of the membrane increases with the SSA content, the methanol permeability also increases, due to the SSA exerting an adverse steric effect on the second crosslinking reaction between GA and PVA-OH [19]. Here a modified two-step crosslinking strategy is proposed to overcome the drawbacks noted in our previous work for the preparation of a PVA-based membrane. Since the second crosslinking reaction between GA and PVA-OH is sterically hindered if the content of SSA is too high, an appropriately lower SSA/PVA-OH ratio was chosen in this work. We introduced the poly(styrene sulfonic acid) (PSSA) as a sulfonating long chain molecular to increase the density of the tangled IPN structure that simultaneously impedes MeOH permeation, while enhancing the proton conductivity of the membrane. The effects of varying amounts of PSSA addition on proton conductivity and on the methanol permeability of the prepared membranes are shown below.

2. Experimental

2.1. Materials and membrane preparation

The membranes were formed using a solution-casting method. The stock PVA (99% hydrolyzed; average M_w = 124,000–186,000; Aldrich) solution was prepared by dissolving PVA (5 g) in DI water (ca. 80 mL) and then heating at 70 °C with continuous stirring until a transparent solution was obtained. Various amounts of PSSA (18 wt%; average M_w = 240,000; Aldrich) were then added to this solution and stirred until uniform. The PSSA/PVA (g g^{-1}) ratios were 0.36 (1-PVA–PSSA), 0.54 (2-PVA–PSSA), 0.72 (3-PVA–PSSA), 0.9 (4-PVA–PSSA), and 1.33 (5-PVA–PSSA).

2.1.1. First chemical crosslinking of PVA–PSSA–SSA

SSA–SO_3H (22 mol% relative to PVA-OH) was added to the above solutions, which were then heated at ca. 70 °C with continuous stirring for at least 6 h. The solutions produced were cast onto plastic dishes and dried in an oven at 38 °C until visually dry. The resulting semi-IPN thin-membranes were then peeled from the plastic substrate.

2.1.2. Second chemical crosslinking of PVA–PSSA–SSA

Samples of the semi-IPN polymer membranes were separately soaked in 0.5 M GA in acetone. Crosslinking occurred between the hydroxyl (OH) groups of PVA and the aldehyde groups of GA, catalyzed by the sulfonic acid units of SSA and PSSA. Acetal groups formed during this second crosslinking process, performed for 1 h (denoted C1). The membranes were washed with acetone and placed in a vacuum oven at 35 °C for 2 h of heat treatment (denoted H2).

2.2. Infrared spectra

The infrared (IR) spectra of the semi-IPN polymer membranes were recorded using an ATR IR spectrometer. Attenuated total reflectance (ATR) IR spectra of the membranes were recorded using a MIRacle single reflection horizontal ATR (HATR) spectrometer (PIKE Technologies). The accessory sampling plate, which comprised two configurations of polished ZnSe crystals, facilitated the reliable analysis of samples. The membrane was squeezed between the ZnSe crystals and a pressing counterpart device, using a micrometer-controlled compression clamp to achieve perfect contact.

2.3. Thermal analysis

Thermal analysis of the semi-IPN polymer membranes was performed by differential scanning calorimetry (DSC) and thermogravimetric analysis (TGA) using respectively DSC-6200 and TG/DTA-6200 instruments, supplied by SII Nano Technology. All measurements were performed using samples under a N_2 environment. TGA data revealed the samples' thermal degradation onset temperatures, which served as reference values for the DSC measurements. DSC of the membranes was performed in a dry N_2 atmosphere at temperatures from 25 to 250 °C. The samples (ca. 5 mg) were placed in aluminum pans and then heated to the desired temperature at a rate of 10 °C min^{-1} for TGA and 5 °C min^{-1} for DSC. The vacant aluminum pan served as a reference throughout the entire set of experiments.

2.4. Swelling of the membranes

The swelling of the semi-IPN polymer membranes was evaluated in terms of their water uptake (WU (g g^{-1})), which was estimated from the change in mass before and after complete drying of the membrane. The membranes were first soaked in distilled water for more than 2 days. They were then removed from the water, carefully wiped clean with a piece of filter paper (or wipe paper), and immediately weighed. Next, the membranes were dried in a vacuum oven at 80 °C for more than 48 h. The WU was calculated using the equation:

$$\mathrm{WU} = \frac{W_{\mathrm{wet}} - W_{\mathrm{dry}}}{W_{\mathrm{dry}}}$$

where W_{wet} and W_{dry} are the masses of the water-swollen and dry membranes, respectively.

2.5. Ion exchange capacity

The ion exchange capacity (IEC) of the semi-IPN polymer membranes was measured using a previously reported titration method [12,19,20]. Pieces of each membrane were soaked in 2 M NaCl (30 mL) for at least 48 h to replace the protons with Na^+ ions. The remaining solution was then titrated with 0.1 M NaOH, using phenolphthalein as an indicator. The IEC is expressed as milliequivalents of SO_3H and COOH groups per gram of dried sample (mequiv g^{-1}).

2.6. States of water

Two types of water, freezing and nonfreezing water (bound water), were detected in the membranes from their melting transitions in the DSC measurements, as described previously [19,21,22]. The samples were first cooled from +25 to −40 °C (cooling rate: 10 °C min^{-1}) and then heated to +40 °C (heating rate: 2 °C min^{-1}). The amount of bulk water in the samples was calculated by integrating the peak area of the melt endotherm. The water's degree of crystallinity, obtained from the heat of fusion of pure ice (334 J g^{-1}), was used as a standard [12,19,21,22].

2.7. Proton conductivity

The proton conductivity (σ) of the polymer membranes was measured using an ac impedance technique employing an electrochemical impedance analyzer (S-1260, Solartron); the ac frequency was scanned from 1000 Hz to 1 MHz at a voltage amplitude of 10 mV. Fully hydrated membranes were sandwiched into a conductivity electrode equipped with Pt foil. The impedance was measured at a steady temperature of 30 °C.

2.8. MeOH permeability

The MeOH permeability of the electrolytes was determined using an in-house fabricated side-by-side diffusion cell. Before measuring the MeOH permeation, the membrane was immersed in pure water at least for 2 days. The membrane was then clamped between the well-stirred donor (chamber A) and receptor (chamber B) compartments (each chamber volume = 100 mL), having a membrane cross-sectional area of 0.7854 cm^2 exposed to the solutions in both the compartments. Chamber B was filled with water, while chamber A was filled with the 1 M MeOH solution; the MeOH concentration in chamber B was determined by measuring the refractive index (RI) at different times [19,23]. The MeOH permeability was then calculated from the curve of the MeOH concentration versus time function.

3. Results and discussion

3.1. Structure of PVA–PSSA–SSA–GA membrane

The esterized crosslinking reaction between the OH of PVA and the COOH of SSA was used for the preparation of our semi-IPN polymers, i.e. to form a primitive network membrane. The SO_3H groups of SSA and PSSA as well as the OH groups of PVA are hydrophilic. When the SO_3H content is high (and the ratio of SO_3H/PVA-OH exceeds 10 mol%), the primitive membrane is soluble in water [19]. Since the SO_3H content was higher than 22%, the primitive membrane was subjected to the subsequent second-step of crosslinking PVA with GA to improve its water resistance [19]. Acetal units were generated over most of the of the membrane's outer surface, thereby forming a protective hydrophobic layer. The membrane was shown to become water-insoluble even when the SO_3H/PVA-OH ratio exceeded 45 mol%. As proof, we immersed the membrane in DI water for ca. 300 days; the water remained clean, while the weight of membrane remained unchanged. This two-step crosslinking process yielded semi-IPN polymer membranes that were highly stable in water. This process also improved the proton conductivity and prevented MeOH cross-over, as described in the following section. Scheme 1 depicts the possible structure of the PVA–PSSA–SSA–GA membranes obtained through the two-step crosslinking strategy.

Table 1
Assignments of the signals in the ATR-IR spectra (500–4000 cm^{-1}) of the PVA–PSSA–SSA–GA membranes.

Assignments	Wave no.
$\omega(-CH_2)_2$	550–660 s
$\upsilon(-CH_2)$	707 sh, m
$\upsilon(-CH=)$	670 w
$\upsilon(-CH=)$	776 w
$\upsilon(C-S)$	803 vow
$\upsilon(C-S)$	840 m
$\upsilon_s(C-O-C)$	970 vow
$\upsilon(-CH=)$	1007 m
$\upsilon(C-O-C)$	1125 m
$\upsilon_s(SO_3^-)$, $(-CH=)$	1037 vs
$\upsilon(C-O-C)$, $\upsilon_{as}(SO_3^-)$	1164 vs
$\upsilon(C-O-C)$, $\upsilon_s(SO_3H)$	1214 vs
$\upsilon_s(SO_3H)$	1224 vs
$\upsilon(C-C)$	1314 sh, m
$\delta(CH)$	1350 sh, m
$\delta(OH)$	1632 sh
$\upsilon(C=O)$	1717 s
$\upsilon_s(CH_2)$	2920 s
$\upsilon_s(CH_2)$	2940 s
$\upsilon(-CH=)$	3000 m, b
$\upsilon(OH)$	3242 vs, b
$\upsilon(OH)$	3406 vs, b

s: strong; m: medium; w: weak; sh: shoulder; v: very; b: broad.
δ: scissoring vibration; ω: wagging and rocking vibration.
υ: vibration; υ_s: symmetry vibrations; υ_{as}: asymmetry vibrations.

3.2. IR spectra of PVA–PSSA–SSA–GA membranes

Table 1 presents the ATR IR spectral vibration mode assignments of PVA–PSSA–SSA–GA membranes containing 22 mol% SSA/PVA-OH and PSSA/PVA (g g^{-1}) contents of: 0.36 (1-PVA–PSSA–SSA–GA-C1H2), 0.54 (2-PVA–PSSA–SSA–GA-C1H2), 0.72 (3-PVA–PSSA–SSA–GA-C1H2), 0.9 (4-PVA–PSSA–SSA–GA-C1H2), and 1.33 (5-PVA–PSSA–SSA–GA-C1H2).

All of the membranes were crosslinked with GA for 1 h and then heat-treated for 2 h. The fingerprint signals of the PVA–PSSA–SSA–GA membrane at 550–660 cm^{-1} are attributed to wagging and rocking vibrations of the $(-CH_2)_2$ units. The peaks at 670, 776, and 1007 cm^{-1} correspond to benzene ring –CH= vibrations. The peak at 707 cm^{-1} corresponds to the CH_2 vibration, and the weak signal at 840 cm^{-1} is assigned to the C–S stretching vibration [4]. The peak at 1125 cm^{-1} corresponds to C–O–C stretching vibrations [4]. We attribute the peak at 1037 cm^{-1} to a combination of symmetric vibration of the SO_3H groups [4] and C–H bending of the benzene rings. Unfortunately, asymmetric vibrations representing SO_3^- group asymmetry, expected at ca. 1164 cm^{-1} were obscured by the intense C–O–C stretching vibration and could not be located precisely. The peaks at 1214–1224 cm^{-1} are associated with symmetric stretching vibrations of the SO_3^- groups and stretching vibrations of the C–O–C units [24]. We attributed the signal at ca. 1632 cm^{-1} in the spectrum of the pristine sample to the bending vibrations of OH groups bonded to the SO_3^- groups;

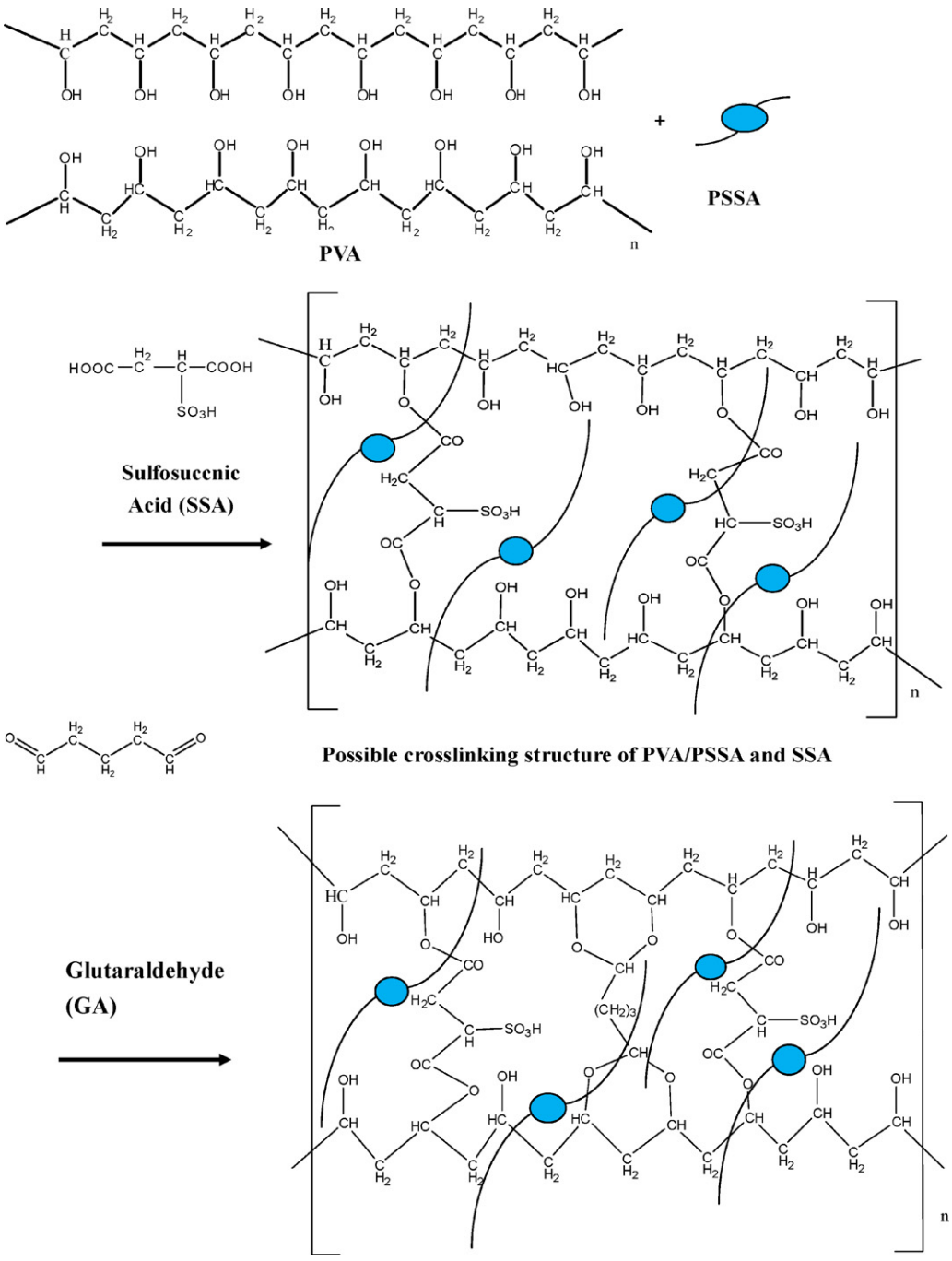

Scheme 1. Schematic semi-IPN structure of the PVA–PSSA–SSA–GA membrane.

this signal indicates that some water molecules were present in the hydrophilic domains of the pristine PVA–PSSA–SSA–GA membrane [24]. The peak at 1717 cm^{-1} in the spectrum of the pristine PVA–PSSA–SSA–GA membrane represents C=O group stretching [19]. The broadening of the peak at 3242–3406 cm^{-1} for the pristine PVA–PSSA–SSA–GA membrane represents the OH group stretching [19].

Fig. 1(a)–(c) presents ATR IR spectra of the PVA–PSSA–SSA–GA membranes. All of the spectral curves were normalized using the peak at 1715 cm^{-1} as a reference since the content of C=O group is unchanged for all the samples. The membranes featuring 22 mol% SSA/PVA-OH and PSSA/PVA ($g\,g^{-1}$) ratios of 0.36, 0.54, 0.72, 0.9, and 1.33 exhibited no spectral characteristics for aldehydic CH groups at 2720 cm^{-1} after the second-step crosslinking of PVA–PSSA–SSA with GA and heat-treatment. The membranes become water-insoluble and their mechanical strength becomes better. This finding confirmed that the second-step crosslinking reaction was complete. Fig. 1(a) reveals peaks at 670, 776, and 1007 cm^{-1} that correspond to the benzene ring –CH= vibrations of PSSA. Fig. 1(b) reveals that the intensity of the signal at 2940 cm^{-1} did not increase upon increasing the PSSA content, whereas that at ca. 3030 cm^{-1} did, due to –CH= vibrations of the benzene rings. The peak at ca. 2852–2858 cm^{-1} corresponds to the –CH vibrations of the acetal units [19]. Fig. 1(b) and (c) reveals that the intensity of the signal at 3242–3406 cm^{-1} increased as the SO_3H/PVA-OH ratio increased. Fig. 1(c) indicates that the intensity of the peak at 3242–3406 cm^{-1} decreased with an increase in the length of time of the second-step crosslinking (i.e. the reaction of GA with PVA), this

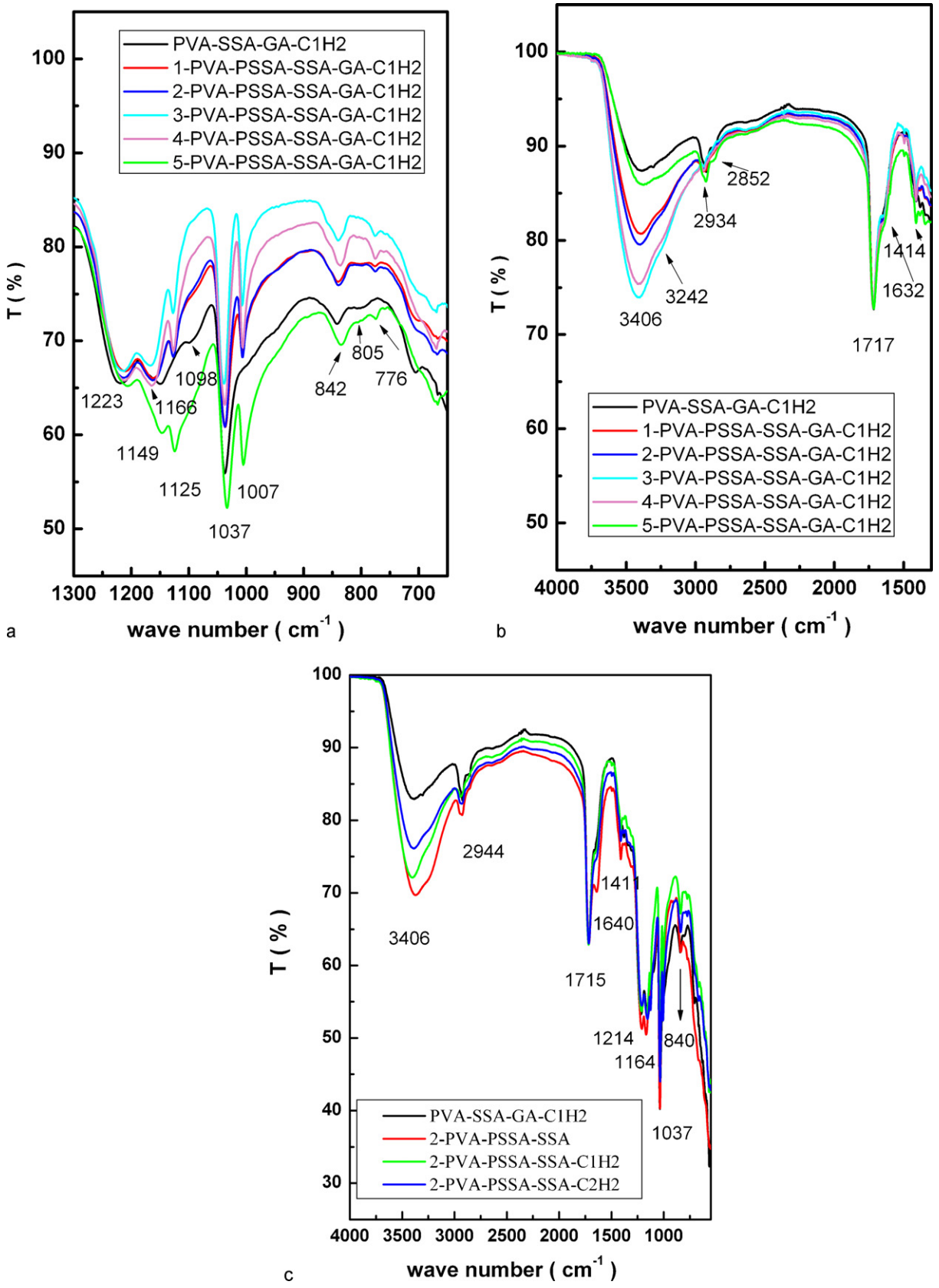

Fig. 1. (a)–(c) ATR IR spectra of membranes made with 22 mol% SSA/PVA-OH and PSSA/PVA ($g\,g^{-1}$) ratios of 0.00, 0.36, 0.54, 0.72, 0.9 and 1.33, after crosslinking with GA for 1 h (denoted C1) or 2 h (denoted C2) and subsequent heat treatment for 2 h (denoted H2): PVA–SSA–GA-C1H2, 1-PVA–PSSA–SSA–GA-C1H2, 2-PVA–PSSA–SSA–GA-C1H2, 2-PVA–PSSA–SSA–GA-C2H2, 3-PVA–PSSA–SSA–GA-C1H2, 4-PVA–PSSA–SSA–GA-C1H2, and 5-PVA–PSSA–SSA–GA-C1H2. The sample 2-PVA–PSSA–SSA was not subjected to crosslinking with GA or heat treatment.

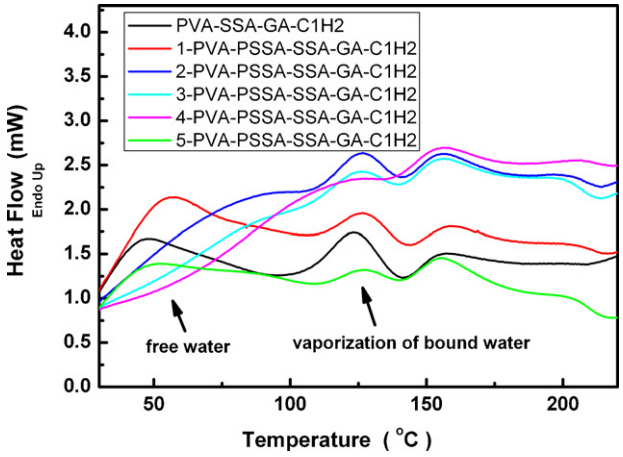

Fig. 2. DSC curves of PVA–PSSA–SSA–GA membranes made with 22 mol% SSA/OH and PSSA/PVA ($g\,g^{-1}$) ratios of 0.00, 0.36, 0.54, 0.72, 0.9, and 1.33. These membranes were crosslinked with GA for 1 h and then subjected to heat treatment for 2 h.

being consistent with the disappearance of the OH groups of PVA. An increase in the PSSA content causes the membranes to become more hydrophilic, which, in turn, leads to higher MeOH permeability [7]. We found, however, that increasing the amount of PSSA led to an increased structural density of the semi-IPN polymer, resulting in the decrease of MeOH permeability and the increase of proton conductivity, water uptake, and the degree of ion exchange (see below).

3.3. Thermal analysis

Fig. 2 presents DSC curves of the PVA–SSA–GA and PVA–PSSA–SSA–GA membranes featuring 22 mol% SSA/PVA-OH and PSSA/PVA ($g\,g^{-1}$) ratios of 0.36, 0.54, 0.72, 0.9, and 1.33. All of these membranes were crosslinked with GA for 1 h and then heat-treated for 2 h. The membranes each exhibited an endothermic heat flow at 50–120 °C. Increasing the PSSA/PVA ($g\,g^{-1}$) ratio caused the curves to shift to higher temperatures, indicating that the presence of additional SO_3H groups led to some previously free water becoming bound water. The endothermic heat flow at 120–140 °C corresponds to vaporized H_2O [19]. The endothermic heat flow at higher temperatures increased with an increase in the PSSA/PVA ($g\,g^{-1}$) ratio, indicating further decomposition of these functional groups.

Fig. 3 presents TGA curves of the PVA–SSA–GA and PVA–PSSA–SSA–GA membranes. All of the membranes were crosslinked with GA for 1 h and then heat-treated for 2 h. Each membrane exhibited a decrease in weight at 40–110 °C, indicating the loss of free water. The weight losses at 120–170 °C correspond to the vaporization of bonded H_2O, while the decreases in weight at 220–340 °C revealed the decomposition of the OH, SO_3, SO_2, and SO_3H units [19]. The weight losses decreased upon increasing the PSSA/PVA ratio. For example, the membranes with PSSA/PVA ($g\,g^{-1}$) ratios of 0.36, 0.54, 0.72, 0.9, and 1.33 showed weight loss of 56.3, 53.8, 52.8, 50.3, 47.4, and 47.2 wt%, respectively at 320 °C. The decreases in weight at 460–520 °C were caused by the decomposition of CH_2 and C_6H_4 units. The reduction in weight loss at a particular temperature upon increasing the PSSA/PVA ratio reveals that the addition of PSSA improved the thermal properties of the membranes.

3.4. Water state and ion exchange capacity

We determined the water states of these semi-IPN polymer membranes from the melting transitions in their DSC traces. Fig. 4

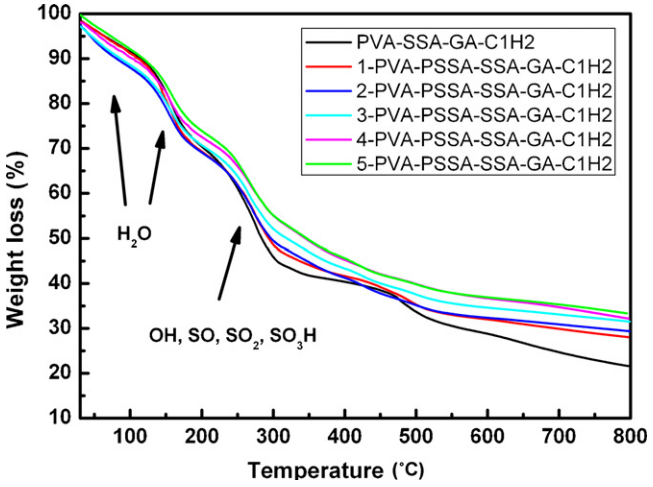

Fig. 3. TGA curves of PVA–PSSA–SSA–GA membranes made with 22 mol% SSA/PVA-OH and PSSA/PVA ($g\,g^{-1}$) ratios of 0.00, 0.36, 0.54, 0.72, 0.9, and 1.33. These membranes were crosslinked with GA for 1 h and then subjected to heat treatment for 2 h.

reveals that the endothermic heat flow, indicative of the amount of freezing water, increased with an increase in the PSSA/PVA ratio [12,19,21,22]. We observed a significant increase in the heat flow at low temperatures, revealing the formation of ice crystals at temperatures from −10 to −20 °C, to be concomitant with an increase in the number of SO_3H groups; to which the water molecules in these ice crystals were bound [19].

Table 2 reveals that increasing the PSSA/PVA ratio in these semi-IPN polymer membranes increased the water uptake, but did not evidently affect the bound-water/free-water ratio. Comparison of the performance of the PVA–SSA–GA and PVA–PSSA–SSA–GA membranes reveals that increasing the PSSA content increased the water uptake and also increased the bound water/free water ratio. Indeed, the degree of water uptake was high and the bound water/free water ratio exceeded that of any previously described PVA-bases electrolyte [6–18]. Table 3 reveals that the ion exchange capacity of the membranes increased upon increasing the PSSA/PVA ratio; interestingly, the optimal ion exchange capacity among our synthesized membranes (2.34 mmol g^{-1}) exceeds that of Nafion. The water uptake and ion exchange capacities of the PVA–PSSA–SSA–GA membranes were good, as were their pro-

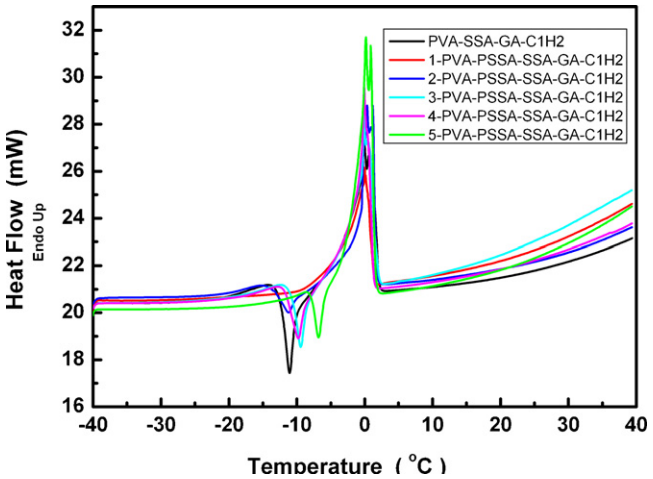

Fig. 4. DSC curves of PVA–PSSA–SSA–GA membranes made with 22 mol% SSA/PVA-OH and PSSA/PVA ($g\,g^{-1}$) ratios of 0.00, 0.36, 0.54, 0.72, 0.9, and 1.33. These membranes were crosslinked with GA for 1 h and then subjected to heat treatment for 2 h.

Table 2
Water-uptake of membranes with various PSSA/PVA ratios.

Sample SSA/PVA-OH = 22 mol%	PSSA/PVA ($g\,g^{-1}$)	Water uptake ($g\,g^{-1}$)	Free water (%)	Bound water (%)
PVA–SSA–GA-C1H2	0.00	0.72	17.02	82.98
1-PVA–PSSA–SSA–GA-C1H2	0.36	1.32	13.86	86.15
2-PVA–PSSA–SSA–GA-C1H2	0.54	1.76	13.57	86.43
3-PVA–PSSA–SSA–GA-C1H2	0.72	1.94	13.94	86.06
4-PVA–PSSA–SSA–GA-C1H2	0.90	2.00	13.73	86.27
5-PVA–PSSA–SSA–GA-C1H2	1.33	2.24	13.50	86.50

Table 3
Methanol permeabilities, proton conductivities and ion exchange capacities of membranes made with various PSSA/PVA ratios.

Sample SSA/PVA-OH = 22 mol%	PSSA/PVA ($g\,g^{-1}$)	Ion exchange ($mmol\,g^{-1}$)	MeOH permeability ($10^{-7}\,cm^2\,S^{-1}$) p	Proton conductivity ($S\,cm^{-1}$) σ	Selectivity σ/p (10^5)
PVA–SSA–GA-C1H2	0.00	1.23	2. 17	0.021	0.968
1-PVA–PSSA–SSA–GA-C1H2	0.36	1.84	3.51	0.027	0.769
2-PVA–PSSA–SSA–GA-C1H2	0.54	1.91	4.58	0.031	0.677
3-PVA–PSSA–SSA–GA-C1H2	0.72	2.05	4.77	0.044	0.922
4-PVA–PSSA–SSA–GA-C1H2	0.90	2.18	3.82	0.046	1.120
5-PVA–PSSA–SSA–GA-C1H2	1.33	2.34	1.68	0.0588	3.500
PVA			29.0	0.0001	
Nafion 117		0.91[a]	14.9	0.0134	

[a] Data obtained from Ref. [25].

ton conductivities. The ion exchange capacities of most of our membranes were greater than those of most previously described PVA-based electrolytes [6,8,11,12,15–18].

3.5. Proton conductivity and MeOH permeability

Table 3 and Fig. 5 respectively present the MeOH permeability and the proton conductivities of our membranes formed with 22 mol% SSA/PVA-OH together with various PSSA/PVA ($g\,g^{-1}$) ratios. All of these membranes were crosslinked with 0.5 M GA in acetone for 1 h, followed by heat treatment for 2 h at 35 °C. At room temperature, the highest proton conductivity that we observed for our synthesized membranes was $5.88 \times 10^{-2}\,S\,cm^{-1}$ (5-PVA–PSSA–SSA–GA-C1H2), a value that exceeds that of Nafion membranes. The MeOH permeability of each of our synthesized membranes was ca. $1 \times 10^{-7}\,cm^2\,S^{-1}$. The proton conductivity increased with an increase in water uptake and IEC, which results from the increase in the $-SO_3H$ of PSSA. The 4-PVA–PSSA–SSA–GA-C1H2, 5-PVA–PSSA–SSA–GA-C1H2 samples exhibited worse MeOH permeability than did the 2-PVA–PSSA–SSA–GA-C1H2 and 3-PVA–PSSA–SSA–GA-C1H2 samples. This finding indicates that the 4-PVA–PSSA–SSA–GA-C1H2, and 5-PVA–PSSA–SSA–GA-C1H2 samples contained a sufficient amount of PSSA to produce a densely tangled IPN structure, effectively preventing MeOH permeability, thereby generating the best selectivity. The membrane without a semi-IPN structure (i.e. PVA–SSA–GA), prepared by our original two-step crosslinking strategy, exhibited increases in both MeOH permeability and proton conductivity with increasing SSA contents [19]. The long chain molecular structure of PSSA exerts a steric effect on the first-step crosslinking reaction between SSA and PVA-OH, leading to greater MeOH permeability. When the PSSA/PVA ($g\,g^{-1}$) ratio was less than 0.72, the membrane did not have enough 'tangled density' within the IPN structure; thus it exhibited increases in both MeOH permeability and proton conductivity. However, it was found that the PSSA/PVA membrane with PSSA/PVA ($g\,g^{-1}$) greater than 0.72 contained enough PSSA to form densely tangled IPN structures that both effectively prevented MeOH permeability, and facilitated increased proton conductivity.

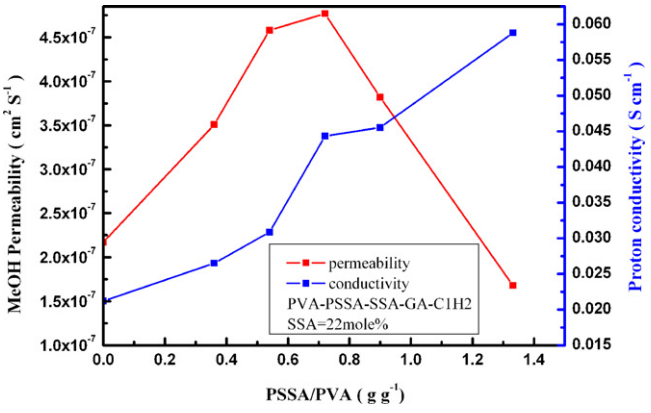

Fig. 5. MeOH permeabilities and proton conductivities of PVA–PSSA–SSA–GA membranes made with 22 mol% SSA/PVA-OH together with PSSA/PVA ($g\,g^{-1}$) ratios of 0.00, 0.36, 0.54, 0.72, 0.9, and 1.33. These membranes were crosslinked with GA for 1 h and then subjected to heat treatment for 2 h.

4. Conclusion

We have introduced PSSA as a sulfonating long chain molecule to prepare PVA-based membranes using a two-step crosslinking strategy. The incorporation of PSSA increased the density of the tangled semi-interpenetrating network (semi-IPN) structure of the membrane that effectively prevents MeOH permeability, while simultaneously increasing the proton conductivity at PSSA/PVA ($g\,g^{-1}$) ratios greater than 0.72. Semi-IPNs based on PSSA/PVA polymer electrolytes, synthesized by a two-step crosslinking process (esterization followed by acetal formation), exhibit excellent properties. The long-chain sulfonating agent used (PSSA) appears not to impede the second-step crosslinking reaction, but rather contributes to the formation of a densely tangled IPN structure that effectively prevents MeOH permeation, while enhancing proton conductivity.

Acknowledgment

We thank the National Science Council for financial support (contracts NSC96-2221-E-011-061 and NSC96-2120-M-011-001), and the National Synchrotron Radiation Research Center (NSRRC), together with the National Taiwan University of Science and Technology, Taiwan, ROC, for the use of facilities and equipment.

References

[1] J.J. Sumner, S.E. Creager, J.J. Ma, D.D. DesMarteau, J. Electrochem. Sci. 145 (1998) 107–110.
[2] S. Slade, S.A. Campbell, T.R. Ralph, F.C.J. Walsh, J. Electrochem. Sci. 149 (2002) 1556–1564.
[3] C.E. Tsai, B.J. Hwang, Fuel Cells 07 5 (2007) 408–416.
[4] A. Gruger, A. Regis, T. Schmatko, P. Colomban, Vib. Spectrosc. 26 (2001) 215–225.
[5] Y.F. Lin, C.Y. Yen, C.C.M. Ma, S.H. Liao, C.H. Lee, Y.H. Hsiao, H.P. Lin, J. Power Sources 171 (2007) 388–395.
[6] H. Akita, K.K. Honda, G. Kenkyusho, W.S. Saltama, 351-0193(JP) E. P. Pat. 1085051 (2001).
[7] J.W. Rhim, H.B. Park, C.S. Lee, J.H. Jun, D.S. Kim, Y.M. Lee, J. Membr. Sci. 238 (2004) 143–151.
[8] R.K. Nagarale, G.S. Gohil, V.K. Shahi, R. Rangarajan, Macromolecules 37 (2004) 10023–10030.
[9] T. Uragami, K. Okazaki, H. Matsugi, T. Miyata, Macromolecules 35 (2002) 9156–9163.
[10] D.S. Kim, H.B. Park, J.W. Rhim, Y.M. Lee, J. Membr. Sci. 240 (2004) 37–48.
[11] D.S. Kim, H.B. Park, J.W. Rhim, Y.M. Lee, Solid State Ionics 176 (2005) 117–126.
[12] T. Qiao, T. Hamaya, T. Okada, Chem. Mater. 17 (2005) 2413–2421.
[13] W. Charles, J. Wolker, J. Electrochem. Sci. 151 (2004) 1797–1803.
[14] C.K. Yeom, K.H. Lee, J. Membr. Sci. 109 (1996) 257–265.
[15] M.S. Kang, J.H. Kim, J. Won, S.H. Moon, Y.S. Kang, J. Membr. Sci. 247 (2005) 127–135.
[16] D.S. Kim, M.D. Guiver, S.Y. Nam, T.I. Yun, M.Y. Seo, S.J. Kim, H.S. Hwang, J.W. Rhim, J. Membr. Sci. 281 (2006) 156–162.
[17] C.W. Lin, Y.F. Huang, A.M. Kannan, J. Power Sources 164 (2007) 449–456.
[18] C.W. Lin, Y.F. Huang, A.M. Kannan, J. Power Sources 171 (2007) 340–347.
[19] C.E. Tsai, C.W. Lin, B.J. Hwang, J. Power Sources 195 (2010) 2166–2173.
[20] C. Manea, M. Mulder, J. Membr. Sci. 206 (2002) 443–453.
[21] L.E. Karlsson, B. Wesslen, P. Jannasch, Electrochim. Acta 47 (2002) 3269–3275.
[22] D.I. Ostrovskii, L.M. Torell, M. Paronen, S. Hietala, F. Sundholm, Solid State Ionics 97 (1997) 315–321.
[23] S.P. Tung, B.J. Hwang, J. Membr. Sci. 241 (2004) 315–323.
[24] R. Buzzoni, S. Bordiga, G. Ricchiardi, G. Spoto, A. Zecchina, J. Phys. Chem. 99 (1995) 11937–11951.
[25] K.D. Kreuer, J. Membr. Sci. 185 (2001) 29–39.